Wiener filter on image quality: a basal ganglia phantom study simulating [I-123] dynamic SPECT imaging [Abstract]. *J Nucl Med* 1993;34(suppl):190.
30. Chang LT. A method for attenuation correction in radionuclide computed tomography. *IEEE Trans Nucl Sci* 1978;NS-25:638–643.
31. Resnick SR, Karp JS, Turetsky BI, Gur RE. Comparison of anatomically defined versus physiologically based regional localization: effects on PET-FDG quantitation. *J Nucl Med* 1993;34:2201–2207.
32. Antonini A, Leenders KL. Dopamine D2 receptors in normal human brain: effect of age measured by PET and [^{11}C]-raclopride. *Ann New York Acad Sci* 1993;695:81–85.
33. Antonini A, Leenders KL, Reist H, Thomann R, Beer HF, Locher J. Effect of age on D2 dopamine receptors in normal human brain measured by PET and ^{11}C-raclopride. *Neurology* 1993;50:474–480.
34. Martin WRW, Palmer MR, Patlak CS, Calne DB. Nigrostriatal function in man studied with PET. *Ann Neurol* 1989;26:535–542.
35. Sawle GV, Colebatch JG, Shah A, et al. Striatal function normal aging: Implications for Parkinson's disease. *Ann Neurol* 1990;28:799–804.
36. Cordes M, Snow BJ, Cooper S, et al. Age-dependent decline of nigrostriatal dopaminergic function: a PET study of grandparents and their grandchildren. *Ann Neurol* 1994;36:667–670.
37. Vingerhoets FJG, Snow BJ, Lee CS, Schulzer M, Mak E, Calne DB. Longitudinal fluorodopa PET studies of the evolution of idiopathic Parkinsonism. *Ann Neurol* 1994;36:759–764.
38. Eidelberg D, Takikawa S, Dhawan V, et al. Striatal fluorine-18-DOPA uptake: absence of an aging effect. *J Cereb Blood Flow Metab* 1993;13:881–888.
39. Choi BC. Definition, sources, magnitude, effect modifiers and strategies of reduction of the healthy worker effect. *J Occup Med* 1993;35:890–892.
40. Blanc PD, Katz P, Yelin E. Mortality risk among elderly workers. *Am J Industrial Med* 1994;26:543–547.
41. Arrighi MH, Hertz-Picciotto I. The evolving concept of the healthy worker survivor effect. *Epidemiology* 1994;5:189–196.
42. Kim H-J, Mozley PD, McElgin W, et al. In vivo quantification of presynaptic dopamine transporter binding parameters in human brains with [I-123]IPT SPECT [Abstract]. *J Nucl Med* 1995;36(suppl):125P.
43. Kim H-J, Mozley PD, Kung M-P, et al. Absolute activity measurements of in vivo monkey brain using a triple-headed SPECT and a new radioligand: [I-123]IPT [Abstract]. *J Nucl Med* 1995;36(suppl):178–179.
44. Kushner SA, Frederick D, Kung M-P, et al. Quantitative [I-123]IPT SPECT measurements: comparisons with ex vivo dissection and in vitro binding assays in nonhuman primates [Abstract]. *J Nucl Med* 1996;37(suppl):66P.

Prediction of Radiation Doses from Therapy Using Tracer Studies with Iodine-131-Labeled Antibodies

Diane A. DeNardo, Gerald L. DeNardo, Aina Yuan, Sui Shen, Sally J. DeNardo, Daniel J. Macey, Kathleen R. Lamborn, Marc Mahe, Mark W. Groch and William D. Erwin

Department of Internal Medicine, University of California Davis Medical Center, Sacramento, California; Department of Radiation Physics, MD Anderson Cancer Center, Houston, Texas; Brain Tumor Research Center, University of California San Francisco, San Francisco, California; Rush-Presbyterian St. Lukes Medical Center, Rush University, Chicago, Illinois; Siemens Medical Systems, Nuclear Medicine Engineering, Hoffman Estates, Illinois

Tracer pharmacokinetic studies are often used in treatment planning for radionuclide therapy including radioimmunotherapy. This study evaluates the validity of using tracer studies to predict radiation doses from therapy with the same radiolabeled antibody. **Methods:** Quantitative imaging and blood radioactivity were used to obtain the pharmacokinetics and radiation doses that were delivered to the total body, blood, marrow, lungs, liver, kidneys, thyroid, spleen and tumors. Tracer and therapy data for eight patients with lymphoma and one patient with breast cancer were compared using linear regression statistics. Doses of ^{131}I-labeled antibody for the tracer studies ranged from 0.1 to 0.4 GBq (2 to 10 mCi), and therapy doses ranged from 0.7 to 5.6 GBq (20 to 150 mCi). **Results:** Radiation doses to tissues and, in particular, the bone marrow and tumors were reliably predicted from tracer studies. In this group of patients, median dose to marrow from marrow targeting, total body and blood was 9.2 cGy/GBq for tracer studies and 7.6 cGy/GBq for therapy studies with a median difference of 0.5 cGy/GBq. Median dose to tumors was 81.1 cGy/GBq for tracer studies and 70.3 cGy/GBq for therapy studies with a median difference of 5.9 cGy/GBq. **Conclusion:** In these patients, tracer studies were predictive of the radiation doses from therapy for total body, major organs and tumors. The radiation doses to marrow and tumors, which are the usual determinants of the therapeutic index, correlated well between tracer and therapy studies ($r \geq 0.95$).

Key Words: iodine-131; radioimmunotherapy; antibody; radiation dosimetry; treatment planning; therapeutic nuclear medicine

J Nucl Med 1996; 37:1970–1975

Radionuclide therapies, such as radioimmunotherapy, require treatment planning that would be improved if radiation doses from the therapeutic dose could be predicted from a tracer dose. Radiation doses depend on pharmacokinetics that may be unique for each patient as well as for each radiopharmaceutical. For example, radiation dose to normal marrow cells incident to targeting of ^{131}I-labeled antibody on malignant cells in the marrow is unique for each patient (*1*).

Protocols that administer marrow-ablative radiation doses have utilized imaging data from tracer studies to determine the antibody and radionuclide dose to be given for subsequent therapy, using a predetermined ceiling on the estimated radiation doses delivered to the critical organs. Eary et al. (*2*) have administered therapy doses of ^{131}I-labeled antibody as large as 22.2 GBq (600 mCi) that delivered up to 1500 cGy to normal organs. Tracer studies were used to select for treatment those patients that showed favorable tumor-to-nontumor localization of the radiolabeled antibody and to determine the amount of antibody and of ^{131}I to be administered.

Tracer studies would be very useful to predict radiation doses from therapy if the pharmacokinetics are the same for tracer and therapy amounts of the radiopharmaceutical (*3*); equivalence has not been documented adequately yet for radiolabeled antibodies. The purpose of this study was to assess the predictive value of the tracer data for the dosimetry of the therapy dose.

MATERIALS AND METHODS

Patients

Patients were selected for this study from a larger group of patients treated with ^{131}I-labeled Lym-1 or ChL6 antibodies because: (a) imaging and blood data commencing immediately after injection were available for 7 days for both the tracer and the therapy studies; (b) the same amount of antibody preload was used

Received Nov. 14, 1995; revision accepted Apr. 4, 1996.
For correspondence or reprints contact: Gerald L. DeNardo, MD, 1508 Alhambra Blvd., Rm. 214, Sacramento, CA 95816.

TABLE 1
Statistical Analysis of Tracer Prediction of Absorbed Radiation Dose for Iodine-131-Labeled Antibody Therapy*

Tissue	Correlation coefficient	Intercept: Point estimate (rads/mCi)	Intercept: 95% confidence interval†	Slope: Point Estimate	Slope: 95% confidence interval†	Residual†‡ (rads/mCi)
Total body	0.82	−0.01	−0.95, 0.93	1.06	0.42, 1.70	−0.22, 0.23
Blood	0.87	−0.03	−0.03, −0.03	1.21	0.60, 1.82	−0.60, 0.76
Marrow targeting	>0.99	0.01	0.01, 0.01	0.97	0.90, 1.04	−0.02, 0.05
Total marrow§	0.95	0.02	0.01, 0.03	1.03	0.69, 1.37	−0.15, 0.29
Lungs	0.99	−0.10	−0.11, −0.09	1.03	0.88, 1.18	−0.12, 0.27
Liver	0.53	0.45	−0.82, 1.72	0.48	−0.19, 1.72	−0.35, 0.27
Kidneys	0.79	0.13	−0.13, 0.39	0.99	−0.07, 2.05	−0.33, 0.64
Thyroid	0.79	0.08	−1.02, 1.18	0.91	0.11, 1.71	−1.73, 1.20
Spleen	0.94	−0.23	−0.44, −0.02	1.10	0.71, 1.49	−0.99, 0.63
Tumor	0.98	−1.04	−1.29, −0.79	1.27	0.91, 1.63	−0.66, 0.42

*Based on matched pairs of tracer and therapy data for each patient.
†Lower bound, upper bound.
‡Difference between predicted and actual therapy values in individual patients.
§Contributions from total-body penetrating radiations, blood and marrow targeted nonpenetrating radiation.

for the tracer and therapy studies; (c) the specific activities of the tracer and therapy radiopharmaceutical doses were comparable; and (d) there was no drug or other apparent source of biologic change likely to alter the pharmacokinetics. Each patient was negative for human anti-mouse antibody (HAMA) before each dose (*4*) and had no other therapy for their malignancies for at least 4 wk before study entry. Seven patients with advanced non-Hodgkins lymphoma (NHL), one with chronic lymphocytic leukemia (CLL) and one with breast cancer were included. Reactivity of malignant tissue with the treatment antibody was documented by immunophenotyping. Eight of the nine patients had tumors that were detected by imaging after both the tracer and therapy doses. One patient (Patient 8) had a complete remission in the interval between therapy and imaging doses.

Prestudy Evaluation

Tumor sizes and volumes were determined from either x-ray CT images of deep tumors using the summation method (*5*) or caliper measurements of superficial tumors assumed to be spheres. Informed consent in accordance with institutional and regulatory agencies was obtained before the study. Before injection of radiolabeled antibody, and on at least 4 subsequent days, 0.5 to 1 ml of Lugol's solution (500 mg/ml) or a saturated solution of potassium iodide (830 mg/ml) was administered orally to the patients to block thyroid uptake of [^{131}I]-iodide.

Radiopharmaceuticals

Lym-1 is an IgG2a isotype, mouse monoclonal antibody that is specific for B-cell malignancies (*6,7*). Lym-1 was produced in our laboratory (*8*) or obtained from Damon Biotech, Inc. (Needham Heights, MA) or Techniclone, Inc. (Tustin, CA) according to specifications. L6 is an IgG2a isotype, mouse monoclonal antibody that targets human adenocarcinoma cells of the breast (*9*). A chimeric human-mouse antibody (ChL6) was produced using recombinant DNA technology in which mouse constant domains were replaced by the human constant domains (*10*).

Lym-1 and ChL6 were iodinated using the chloramine-T method. Immunochemical analyses confirmed that at least 90% of the radioactivity was associated with the antibody. Immunoreactivity of each ^{131}I-Lym-1 preparation was at least 87% and the ^{131}I-ChL6 preparation was at least 75% (*11*). All radiopharmaceutical products were documented to be sterile and pyrogen-free. The ^{131}I-Lym-1 radiopharmaceutical contained 0.037 to 0.37 GBq (1 to 10 mCi) of ^{131}I per mg of antibody. The ^{131}I-ChL6 radiopharmaceutical contained 0.37 GBq (10 mCi) of ^{131}I per mg of antibody.

Antibody Infusion

The interval between tracer and therapy doses was 1 wk in three patients, 2 wk in one patient, 4 wk in four patients and 6 mo in one patient (Patient 8). Tracer doses ranged from 0.07 to 0.37 GBq (2 to 10 mCi) and therapy doses from 0.74 to 5.55 GBq (20 to 150 mCi) ^{131}I. Before ^{131}I-labeled antibody, unlabeled (preload) Lym-1 or L6 was given in amounts sufficient to saturate isotype-specific receptors or antigen on normal cells (*12,13*) and ranged from 4 to 20 mg for patients with lymphoma except for the patient with CLL, in which a preload has not proven necessary because the antibody targets circulating lymphocytes. The patient with breast cancer received a preload of 200 mg before each dose. The amount of preload antibody was the same for tracer and therapy studies in each patient. However, the amount (mg) of antibody in the tracer dose differed from that in the therapeutic dose because the specific activity (mCi/mg) of the radiopharmaceutical was kept relatively constant and the amounts of ^{131}I (mCi) were different. The total amounts of antibody ranged from 5 to 21 mg for tracer studies and from 7 to 27 mg for therapy studies in patients with NHL. The patient with CLL received a total of 0.2 mg for the tracer study and 2 mg for therapy, and the patient with breast cancer received a total of 201 mg for the tracer study and 215 mg for therapy.

Analysis of Tracer Prediction of Radiation Dose from Therapy

Radiation doses to total body, blood, marrow, lungs, liver, kidneys, thyroid, spleen and tumors were compared for tracer and therapy doses of ^{131}I-labeled antibody to evaluate the ability to predict the radiation dose from therapy, using the data obtained from the tracer study. Statistical methods (*14*) included linear regression of radiation doses to total body, organs and tumors obtained for matched pairs of tracer and therapy doses. Linear regression provided correlation coefficients, slopes and intercepts that represent closeness of association, direction and magnitude of the association and displacement of the association respectively. The width of confidence limits for the slope and intercept of each regression line provide an indication of the precision of the estimate. If a slope is nonzero, a correlation exists. Therefore, no separate testing was done on the correlation coefficient (Table 1).

The differences in results for tracer and therapy studies in

individual patients were determined by subtracting each result for the therapy study from the corresponding result for the tracer study. To determine whether there was a relationship between the radiation dose to total body or to blood and the injected radioactivity, the total body and blood radiation doses were compared with the amount of injected ^{131}I.

Radiation Dosimetry

A dosimetry software program, based on the MIRD approach, was used to obtain radiation doses from cumulated activities derived from pharmacokinetic data (*15*). Methods for determining radiation dose to the total body have been previously described (*16*). Cumulated radioactivity in the body was converted to radiation dose estimates using the S value for ^{131}I penetrating and nonpenetrating emissions from MIRD (*15*). Radiation contributed to the blood from nonpenetrating ^{131}I emissions in the blood were estimated by methods previously described (*17*). Radiation doses to organs were obtained using the S factor for penetrating and nonpenetrating radiations. For this study, radiation doses for tumors were estimated using an S factor for nonpenetrating radiations that was derived from MIRD formulations using nonpenetrating energy depositions and the tumor mass (*18*).

Radiation to the bone marrow was analyzed for each of three contributing sources: total body, blood and specific marrow targeting (*19*). The S value for penetrating ^{131}I emissions, assuming a uniform distribution of radionuclide in the body, was obtained by separating the S values for nonpenetrating and penetrating emissions using MIRD values (*15,18,20*). To determine the contributions of radiation dose to bone marrow from radioactivity in the blood, the cumulated radioactivity of the blood was adjusted by correcting for the relative masses (volumes) of blood and marrow, and assuming a concentration or specific activity of 0.25 in the marrow when compared to blood (*21*). The S value for nonpenetrating emissions in the marrow blood was used and an absorbed fraction of one was assumed (*20*). Radiation dose to the marrow from specific marrow targeting was determined for nonpenetrating emissions from cumulated activity in the marrow. The cumulated activity in the marrow was determined by extrapolation of the cumulated activity in three lumbar vertebrae to the mass of the entire marrow (*19*).

Pharmacokinetics

Image Acquisition. A transmission image of the patient was acquired and used for attenuation correction of the tracer and therapy images. A line source spanning the width of the patient was attached to the yoke of the camera with a constant distance between the line source and the detector.

Conjugate anterior and posterior, total body and static emission images were acquired, using a Siemens Orbiter 7500 LFOV camera (Siemens Medical Systems, Inc. Hoffman Estates, IL) interfaced to an ADAC System I computer (ADAC Laboratories, Milpitas, CA) or a Siemens Micro/Maxdelta computer, immediately, at 2–6 hr and daily for 7 days after injection of the radiopharmaceutical. Images were acquired using a high-energy, parallel-hole collimator and a 20% energy window centered at 364 keV and were stored in a 128 × 128 word mode matrix in the computer. Static images of the chest, abdomen and pelvis were acquired for 1 million counts or 600 sec, whichever occurred sooner. One million counts were acquired at 24 hr for tracer and therapy studies. On the last day of imaging, greater than 300,000 counts were acquired for therapy and greater than 100,000 counts were acquired for tracer studies on static images that were stopped by acquisition time. Typically, count density in regions of low radioactivity were greater than 60 counts/pixel providing approximately 13% Poisson statistical error.

Blood. Sequential blood samples were assayed for radioactivity, and blood pharmacokinetics and dosimetry were determined as described previously by DeNardo et al. (*17*). Briefly, counts in each sample were converted to ^{131}I concentration and the percentage of the injected dose (% ID) per milliliter was extrapolated to that in the patient's blood volume determined from the patient's weight. The blood-clearance curves derived from these measurements were biexponential in all instances. Computerized biphasic exponential analysis was performed on the blood data to derive biologic half-lives (hr) for a fast (α) phase and a slow (β) phase.

Image Processing. A single operator processed the tracer and therapy studies of an individual patient. Radioactivity in the normal tissues and readily quantifiable tumors in each patient were estimated using serial radionuclide images. Counts in regions of interest (ROIs) on each image were converted to radioactivity to determine pharmacokinetics and radiation doses. ROIs were visually defined by the operator using the best image in the sequence; the same ROI was used for all images in the sequence and for both tracer and therapy studies. Separate ROIs (left and right) were used to define each of the pair of lungs and kidneys, and the calculated % IDs for each pair were added together. If uptake in other tissues was superimposed (e.g., liver superimposed on kidney), a smaller aliquot ROI that excluded radioactivity in the superimposing tissue and a full ROI around the entire organ were defined. Counts per pixel in the aliquot ROI were normalized to the number of pixels in the full ROI. To define ROIs for background subtraction, regions of the body were selected with thickness comparable to that surrounding the organ or tumor. When more than 1.1 GBq (30 mCi) ^{131}I was present in the patient's body, a correction factor for count loss due to coincidence was applied, using a modification of the method of Freedman (*22*), wherein a standard curve was constructed from a comparison of counts in an ^{131}I reference standard imaged with and without the patient in the field of view. The geometric mean (GM) or the effective point source (EPS) approaches were used to calculate radioactivity in tissues from counts in the ROIs. The GM method was used for image quantitation of the total body, liver and spleen because they could be readily defined from anterior and posterior views (*23,24*). The EPS method was used to quantitate radioactivity in the lungs, kidneys, thyroid, marrow and tumors where ROIs could not be readily defined for both of the opposing views (*16,25*). ROIs were defined on posterior images for lungs, kidneys and marrow, on anterior images for thyroid and on the images that best defined the tumors.

Radioactivity was converted to percent injected dose for each time point. A monoexponential linear regression (least squares fit) of percent injected dose compared with time was used to obtain biologic half-lives and cumulated activities for total body, organs and tumors. Tumor uptake of ^{131}I-labeled antibody peaked at 6–24 hr. Therefore, the effect of using a monoexponential curve fit, on the prediction of tumor radiation dose from therapy, was evaluated. The application of a monoexponential curve fit to time-activity curves for tumors, including and excluding imaging data from the first 24 hr was compared for radiation dose.

RESULTS

Analysis of Tracer Prediction of Radiation Dose from Therapy

Linear regression for tracer compared with therapy doses of ^{131}I-Lym-1 and ^{131}I-ChL6 were obtained. Point estimates and confidence limits of the slopes and intercepts of the regression lines for total body, organs and tumors demonstrated statistically significant and direct correlations of radiation doses for tracer and therapy studies as shown by slopes that approximated one and intercepts that were close to zero (*14*) (Table 1). There was a positive association between radiation doses predicted by the tracer studies and the actual radiation doses for the therapy

TABLE 2
Differences between Pairs of Data (Tracer minus Therapy) for Individual Patients Receiving Iodine-131-Lym-1

	Radiation dose difference*		Biologic half-life difference*	
	Median (cGy/GBq)	Range (cGy/GBq)	Median (days)	Range (days)
Total body	0.3	−6.5, 5.1	0.1	−1.0, 1.0
Blood (β phase)	0.3	−27.0, 10.8	<0.1	−0.4, 1.1
Marrow†	−0.3	−1.6, 0.5	0	−3.9, 0
Lungs	1.6	−8.1, 2.7	0	−0.8, 1.3
Liver	0.8	−5.4, 16.2	0	−0.7, 0.6
Kidneys	1.1	−5.4, 5.4	0.1	−0.3, 0.8
Thyroid	10.8	−27.0, 54.0	0.1	−3.8, 3.1‡
Spleen	−2.7	−16.2, 2.7	0	−0.4, 0.4
Tumors	5.4	−32.4, 8.1	0.4	0, 0.6

*Represents the differences between pairs (tracer minus therapy) of data for each patient.

†Uptake in marrow from targeting of marrow constituents.

‡Patient 7 had increasing uptake in the thyroid during the tracer study.

studies ($r > 0.9$ for lungs, spleen, marrow and tumors) with a nonzero slope in all cases except for the liver and kidneys. A slope of one is a possibility in the associations for the liver and kidney because one falls within the slope intervals. In two cases (liver and tumors), the intercepts differed from zero; the ranges of radiation dose values were far from zero for these tissues. Regression lines are expected to fit well within the range of doses studied. In the case of liver and tumors, doses are far from zero. Therefore, extrapolation to a zero dose (intercept) is not of clinical interest. The correlation coefficient for the liver was lower than those of other tissues in this group of patients. The radiation doses to liver for the tracer and therapy studies for Patient 3 were more variant than was the case for other patients in this group; when this patient was excluded, the correlation was closer ($r = 0.83$) and the intercept was 0.09.

The minimum and maximum residuals for individual patients (difference in values between those predicted from the regression and actual therapy) for each tissue ranged from 1.4 to 32 cGy/GBq (0.05 to 1.20 rads/mCi) (Table 1). To determine the effect of the maximum underestimation of radiation dose to normal tissue, we considered a theoretical therapy dose of 5.55 GBq (150 mCi). An underestimation of 32 cGy (1.20 rads) for this therapy dose would not result in unexpected organ toxicity. Under this scenario, applying the greatest overestimation for tumors (−17.8 cGy/GBq, −0.66 rads/mCi), the predicted radiation dose was 540 cGy and the theoretical radiation dose from 5.55 GBq (150 mCi) was 441 cGy. The median residuals were: −0.38, 0.27, −1.17, −0.61 and 2.95 cGy/GBq for total body, liver, lungs, marrow (from body, blood and marrow targeting) and tumors, respectively.

Radiation Dosimetry

Radiation doses to total body, blood, organs and tumors were comparable for tracer and therapy doses of ^{131}I-labeled antibody. The median differences in radiation doses were not more than 14% of the median radiation dose from ^{131}I-Lym-1 therapy to that tissue (Table 2). The thyroid had the largest median difference as a percentage of the radiation dose from therapy (14%). The median difference in radiation dose to the marrow from targeting showed an underestimation (<10%) by the tracer study and the median difference to the tumor showed an overestimation (<7%). The differences in radiation doses between the tracer and therapy studies for the patient that received ^{131}I-ChL6 also fell within the ranges for ^{131}I-Lym-1.

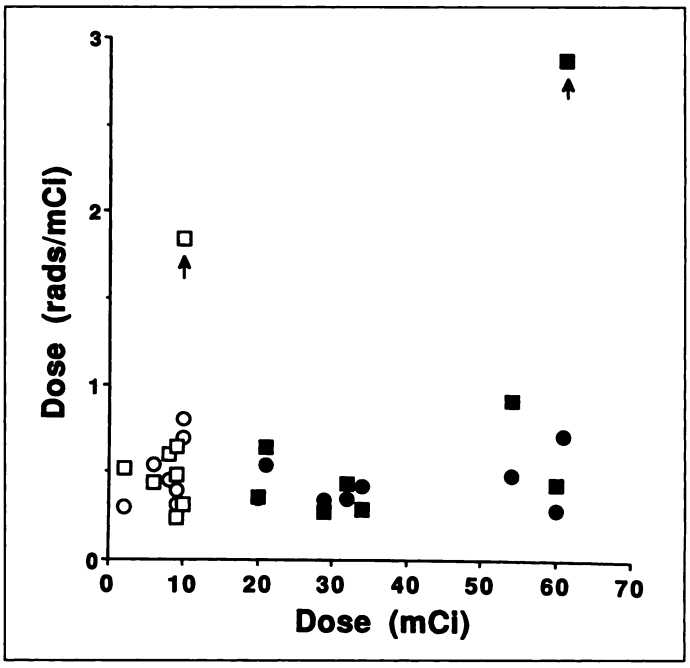

FIGURE 1. Relationship of the amount of injected ^{131}I-Lym-1 to radiation doses to the blood (■) and to the total body (●) from tracer (open symbols) and therapy (solid symbols) doses. One patient (Patient 8) had unusually slow blood clearances for both tracer and therapy doses and resultant higher radiation doses to blood (↑) than the remaining patients. The amount of injected ^{131}I-Lym-1 did not influence radiation dose per unit of administered radioactivity (total body $r = 0.03$, blood $r = 0.16$).

The median radiation dose to tumor from ^{131}I-Lym-1 therapy was 70.3 cGy/GBq (2.6 rads/mCi), and the median radiation dose to marrow from total body, blood and marrow targeting was 8.1 cGy/GBq (0.3 rads/mCi) [range 5.4, 35.1 cGy/GBq (0.2, 1.3 rads/mCi)]. The median therapeutic index, defined as the ratio of tumor to marrow radiation dose in each patient, was 9.5 (range 3.2, 30.8) for this group of patients.

The radiation doses to total body and blood were compared with the amount of injected ^{131}I (mCi) (Fig. 1). The amount of injected ^{131}I did not influence radiation doses to blood ($r = 0.16$) or to total body ($r = 0.03$) per unit of administered radioactivity.

Pharmacokinetics

For individual patients, the results from biexponential analysis of blood clearances for tracer and therapy studies were comparable for biologic half-life (Table 2). For other tissues, the time-activity curves were generally monoexponential (i.e., the log of percent injected dose data fit well with a single straight line using a least squares fit) except for tumors and, occasionally, the spleen and marrow. Although uptake of ^{131}I-labeled antibody in tumor was not monoexponential, application of a monoexponential analysis provided a good approximation of radiation dose (within 15% of that obtained from multiexponential fitting) and a reasonable estimate of biologic half-life (Fig. 2). A monoexponential curve fit to time-activity curves for uptake of ^{131}I-Lym-1 in tumors, including and excluding data from the first 24 hr, was compared for radiation dose. The inclusion or exclusion of data from the first 24 hr did not significantly affect the estimates of radiation dose or mathematical intercept in the tumors studied here when the medians were compared. The median difference in radiation dose to tumors between tracer and therapy studies was 8.1 cGy/GBq (0.3 rads/mCi) and 2.7 cGy/GBq (0.1 rads/mCi)

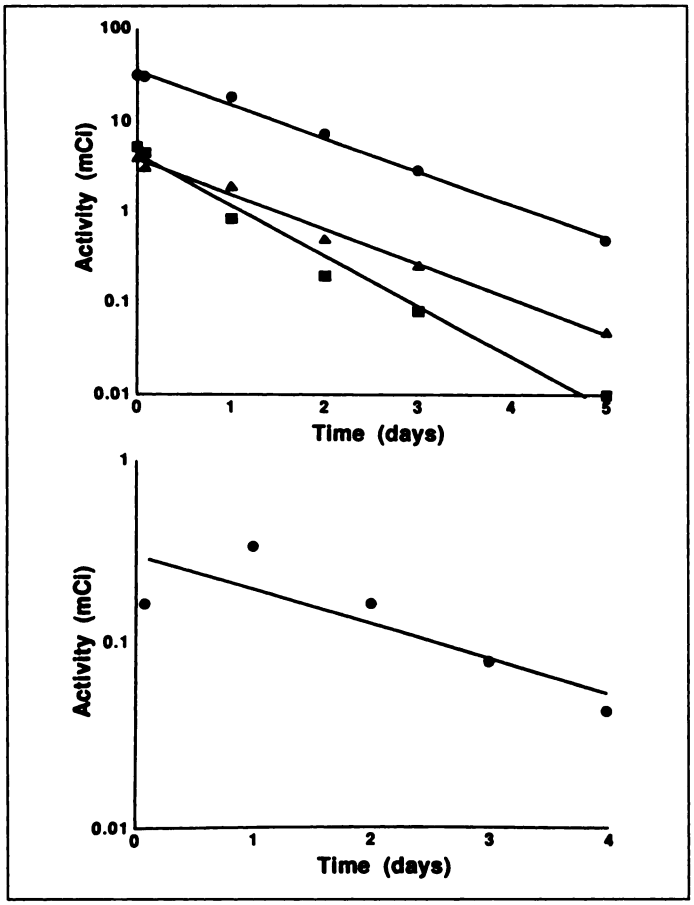

FIGURE 2. Iodine-131-Lym-1 activities (and pharmacokinetics) in the total body (●), liver (■) and lungs (▲) fit a monoexponential clearance pattern (upper) with R values of 0.99 0.99 and 0.98, respectively. ^{131}I-Lym-1 activity in the tumor showed early uptake followed by clearance (lower) that was approximated by a monoexponential fit (r = 0.59) that generated cumulated activity (520 μCi-hr/mCi) comparable to that generated by a multiexponential fit (620 μCi-hr/mCi).

including and excluding the first 24 hr data, respectively. When, monoexponential fitting of the time-activity curves was used for tracer and therapy studies for all tissues except blood, the differences for individual patients between the biologic half-lives of the tracer and therapy doses in tissues were small.

DISCUSSION

In an attempt to validate the use of a tracer study to predict the radiation doses that would be received from therapy, we compared pharmacokinetic and dosimetric data obtained with tracer or therapy doses of ^{131}I-labeled antibodies in patients that had complete blood and image radioactivity analyses over 7 days. This allowed characterization of early and late phases of uptake and clearance of ^{131}I-labeled antibody for both tracer and therapy yielding more complete information for radiation doses and biologic half-lives than that reported by others.

Other investigators have used tracer studies to predict therapeutic doses of ^{131}I in patients (*26,27*). O'Connor et al. (*26*) found that the uptakes and effective half-lives of tracer doses of ^{131}I in the thyroid correlated well with those of therapy doses up to 5.55 GBq (150 mCi) (r = 0.94) in 31 patients with thyrotoxicosis. They also reviewed two related studies and reported that uptakes (104 patients) and effective half-lives (92 patients) were within 20% of each other in all three studies, although comparisons were better for studies with more complete observations. In a study on uptake and dosimetry in patients with thyroid cancer, Maxon et al. (*27*) stated that the effective half-life of ^{131}I in the body for the diagnostic dose correlated with that for the treatment dose (r = 0.8). However, the diagnostic study underestimated the radiation doses to metastases from therapy because a lack of data beyond 72 hr after the diagnostic dose led to the omission of the long-term component of biologic retention found in the therapy study.

Good correlations have been reported for tracer and therapy pharmacokinetics for ^{131}I-labeled antibodies against lymphoma (*2,28*). In three patients, Meredith et al. (*28*) injected tracer doses followed 1 wk later by a therapy dose of ^{131}I-Lym-1 using the same amount of unlabeled antibody preload for the tracer and therapy studies. The tracer studies were predictive of radiation dose from therapy although the early part of the therapy dose pharmacokinetics were not acquired because of radiation safety concerns. Eary et al. (*2*) used imaging and plasma clearance studies to select patients for ^{131}I-labeled anti-pan B-cell antibody therapy. Therapy amounts of the radiolabeled antibody were given to 10 patients in whom the tracer study predicted that the tumors would receive radiation doses equal to or greater than that for any normal organ, excluding bone marrow. Pharmacokinetic data obtained from the therapy studies confirmed that the tracer study accurately predicted the pharmacokinetics of the therapy dose although, again, data were not obtained for the early portions of the therapy study.

In mice, Badger et al. (*29*) found that amounts of ^{131}I-labeled antibody up to the equivalent of a patient dose of 28 GBq (754 mCi, corrected for body surface area) did not alter dosimetry for blood, liver, lung or kidney. However, doses greater than a patient dose of 4 GBq (108 mCi) altered dosimetry for targeted lymph node, marrow, spleen and thymus. In patients, however, Eary et al. (*30*) reported that the clearance half-lives for therapy doses up to 22 GBq (602 mCi) were predicted well from tracer doses of ^{131}I-labeled antibody in patients with leukemia and lymphoma except in one patient who developed a HAMA response that resulted in rapid clearance of the therapy dose.

The use of an antibody labeled with different radionuclides for tracer and therapy doses has been investigated, for example, the use of ^{99m}Tc-labeled antibody as a tracer to predict dosimetry for ^{186}Re-labeled antibody in patients (*31*). Breitz et al. (*31*) used ^{99m}Tc-labeled NR-CO-02 $(Fab')_2$ as a tracer to predict dosimetry from ^{186}Re-labeled NR-CO-02. Rhenium-186 dosimetry could not be reliably predicted for individual patients, probably related to the different antibody masses that were administered for the two studies.

Biologic half-lives are often obtained using a monoexponential fit of the time-activity data (*30,32,33*), as we did here, despite the likelihood that the kinetics are more complex. Peak uptake of ^{131}I-Lym-1 in tumors occurred within the first 24 hr in this group of patients. In this dataset, application of a monoexponential fit to time-activity data that were not absolutely monoexponential yielded equivalent results for radiation dose. Another investigation compared a monoexponential fit to a biexponential fit for time-activity data from 10 tumors; the average difference in results was 14% for ^{131}I-Lym-1 (*34*). Monoexponential curve fitting worked in this situation because there was not a great and prolonged uptake phase for ^{131}I-Lym-1 in the tumors or other tissues.

The prediction by the tracer dose of radiation dose from therapy was validated under defined conditions in this study for ^{131}I-Lym-1 doses up to 2.2 GBq (60 mCi): (a) similar masses of unlabeled antibody were administered before tracer and therapy doses; (b) the interval between doses was relatively short; and (c) similar biologic conditions were present for both studies (e.g., absence of HAMA or other drugs). The radiation dose to

lungs, tumors and marrow from targeting were predicted best ($r \geq 0.98$). The maximum difference in radiation dose to marrow from total body, blood and marrow targeting was an underestimation of 12% of the median radiation dose from therapy.

Tracer studies can be used to plan therapy dose levels in order to give an optimal dose to tumors without seriously suppressing the marrow. In a study by DeNardo et al. (*17*), of 52 patients with B-cell malignancies treated with ^{131}I-Lym-1, myelosuppression manifested by peripheral blood cytopenia was the radiation dose-limiting toxicity. The use of the tracer method should be tested before use in treatment planning with other radioimmunoconjugates. This is particularly critical when the radionuclide for the tracer study is different from that to be used for therapy.

CONCLUSION

Tracer studies of ^{131}I-labeled antibody were predictive of radiation dose from therapy in this group of patients. In particular, the radiation doses to marrow and tumor, which determine the therapeutic index, were predicted well. To the extent that these results can be extrapolated to similar circumstances, it appears legitimate to estimate the suitability of radioimmunotherapy for individual patients from tracer studies conducted in that patient.

ACKNOWLEDGMENTS

We thank Gary Mirick for technical assistance. This research was supported by grants from the Department of Energy (DE-FG03-84ER60233) and the National Cancer Institute (PHS NCI-P01 CA 47829).

REFERENCES

1. DeNardo GL, DeNardo SJ, Macey DJ, Shen S, Kroger LA. Overview of radiation myelotoxicity secondary to radioimmunotherapy using ^{131}I-Lym-1 as a model. *Cancer* 1994;73:1038–1048.
2. Eary JF, Press OW, Badger CC, et al. Imaging and treatment of B-cell lymphoma. *J Nucl Med* 1990;31:1257–1268.
3. DeNardo GL, Raventos A, Hines HH, et al. Requirements for a treatment planning system for radioimmunotherapy. *Int J Radiat Oncol Biol Phys* 1985;11:335–348.
4. DeNardo GL, Kroger LA, Mirick GR, Lamborn KR, DeNardo SJ. Analysis of antiglobulin (HAMA) response in a group of patients with B-lymphocytic malignancies treated with ^{131}I-Lym-1. *Int J Biol Markers* 1995;10:67–74.
5. Breiman RS, Beck J, Korobkin M, et al. Volume determinations using computed tomography. *Am J Roentgenol* 1982;138:329–333.
6. Epstein AL, Zimmer AM, Spies SM, et al. Radioimmunodetection of human B-cell lymphomas with a radiolabeled tumor-specific monoclonal antibody (Lym-1). In: Cavalli F, Bonadonna G, Rozencweig GM, eds. *Malignant lymphomas and Hodgkin's disease: experimental and therapeutic advances*. Boston, MA: Martinus Nijhjoff; 1985:569–577.
7. Epstein AL, Marder RJ, Winter JN, et al. Two new monoclonal antibodies, Lym-1 and Lym-2, reactive with human-B-lymphocytes and derived tumors, with immunodiagnostic and immunotherapeutic potential. *Cancer Res* 1987;47:830–840.
8. DeNardo SJ, Peng J-S, DeNardo GL, Mills SL. Immunochemical aspects of monoclonal antibodies important for radiopharmaceutical development. *Nucl Med Biol* 1986;13:303–310.
9. Hellstrom I, Horn D, Linsley P, Brown JP, Brankovan V, Hellstrom KE. Monoclonal antibodies raised against human lung carcinomas. *Cancer Res* 1986;46:3917–3923.
10. Liu AY, Robinson RR, Hellstrom KE, Murray ED Jr, Chang CP, Hellstrom I. Chimeric mouse-human IgG1 antibody that can mediate lysis of cancer cells. *Proc Natl Acad Sci USA* 1987;84:3439–3443.
11. Beaumier PL, Neuzil D, Yang HM, et al. Immunoreactivity assay for labeled anti-melanoma monoclonal antibodies. *J Nucl Med* 1986;27:824–828.
12. DeNardo GL, DeNardo SJ, O'Grady LF, Levy NB, Adams GP, Mills SL. Fractionated radioimmunotherapy of B-cell malignancies with ^{131}I-Lym-1. *Cancer Res* 1990;50: 1014s–1016s.
13. DeNardo SJ, O'Grady LF, Hellstrom I, et al. Dose-dependent human biokinetics of L-6 MoAb [Abstract]. *J Nucl Med* 1989;30(suppl):907.
14. Sokal RR, Rohlf FJ. *Biometry*. San Francisco, CA: W.H. Freeman; 1969:422.
15. Snyder WS, Ford MR, Warner GC. "S" absorbed dose per unit cumulated activity for selected radionuclides and organs. In: *MIRD pamphlet 11*. New York, NY: Society of Nuclear Medicine; 1978.
16. Macey DJ, DeNardo GL, DeNardo SJ. A treatment planning program for radioimmunotherapy. In: Vaeth, JM, Meyer JL, eds. *Frontiers in radiation therapy oncology*. San Francisco: S. Karger, Basel; 1990: 123–131.
17. DeNardo GL, Mahe MA, DeNardo SJ, et al. Body and blood clearance and marrow radiation dose of ^{131}I-Lym-1 in patients with B-cell malignancies. *Nucl Med Commun* 1993;14:587–595.
18. Loevinger R, Berman M. A revised schema for calculating the absorbed dose from biologically distributed radionuclides. *MIRD pamphlet 1*. New York, NY: Society of Nuclear Medicine; 1976.
19. Macey DJ, DeNardo SJ, DeNardo GL, DeNardo DA, Shen S. Estimation of radiation absorbed doses to the red marrow in radioimmunotherapy. *Clin Nucl Med* 1995;20: 117–125.
20. Dillman LT, Von der Lage F. Radionuclide decay schemes and nuclear parameters for use in radiation-dose estimation. In: *MIRD pamphlet 10*. New York, NY: Society of Nuclear Medicine; 1971.
21. Siegel JA, Wessels BW, Watson EE, et al. Bone marrow dosimetry and toxicity for radioimmunotherapy. *Antibod Immunoconj Radiopharm* 1990;3:213–233.
22. Freedman GS, Kinsela T, Dwyer A. A correction method for high-count rate quantitative radionuclide angiography. *Radiology* 1972;104:713–715.
23. Thomas SR, Maxon HR, Kereiakes JG. In vivo quantitation of lesion radioactivity using external counting methods. *Med Phys* 1976;3:253–255.
24. Hammond ND, Moldofsky PJ, Beardsley MR, Mulhern CB. External imaging techniques for quantitation of distribution of I-131 F(ab')2 fragments of monoclonal antibody in humans. *Med Phys* 1984;11:778–783.
25. DeNardo GL, DeNardo SJ, Macey DJ, Mills SL. Quantitative pharmacokinetics of radiolabeled monoclonal antibodies for imaging and therapy in patients. In: Srivastava SC, ed. *Radiolabeled monoclonal antibodies for imaging and therapy*. New York, NY: Plenum Publishing Corp; 1988: 293–310.
26. O'Connor MK, Cullen MJ, Malone JF. The value of a tracer dose in predicting the kinetics of therapeutic doses of ^{131}I in thyrotoxicosis. *Br J Radiol* 1979;53:719–726.
27. Maxon HR, Thomas SR, Hertzberg VS, et al. Relation between effective radiation dose and outcome of radioiodine therapy for thyroid cancer. *N Engl J Med* 1983;309:937–941.
28. Meredith RF, Khazaeli MB, Plott G, et al. Comparison of diagnostic and therapeutic doses of ^{131}I-Lym-1 in patients with non-Hodgkin's lymphoma. *Antibod Immunoconj Radiopharm* 1993;6:1–11.
29. Badger CC, Davis J, Nourigat C, et al. Biodistribution and dosimetry following infusion of antibodies labeled with large amounts of I-131. *Cancer Res* 1991;51:5921–5928.
30. Eary JF, Pollard KR, Durack LD, et al. Post-therapy imaging in high dose I-131 radioimmunotherapy patients. *Med Phys* 1994;21:1157–1162.
31. Breitz HB, Fisher DR, Weiden PL, et al. Dosimetry of rhenium-186-labeled monoclonal antibodies: methods, prediction from technetium-99m-labeled antibodies and results of phase I trials. *J Nucl Med* 1993;34:908–917.
32. Wahl RL, Zasadny KR, Kaminski MS. Importance of the terminal portion of tumor time-activity curve in determining tumor dosimetry in radioimmunotherapy. *J Nucl Med* 1991;32:1314–1315.
33. Leichner PK, Yang NC, Frenkel TL, et al. Dosimetry and treatment planning for ^{90}Y-labeled antiferritin in hepatoma. *Int J Radiat Oncol Biol Phys* 1988;14:1033–1042.
34. Shen S, DeNardo GL, O'Donnell RT, et al. Practical simplifications for dosimetric models for radioimmunotherapy. *Sixth International Radiopharmaceutical Dosimetry Symposium* 1996: in press.